Influence of a time-periodic magnetic flux on interacting electrons in a one-dimensional loop

Guido Burmeister and Klaus Maschke
Institute of Theoretical Physics, Swiss Federal Institute of Technology, CH-1015 Lausanne, Switzerland
(Received 22 May 2002; revised manuscript received 31 October 2002; published 3 April 2003)

We consider N strongly interacting electrons in a one-dimensional circular loop that is pierced by a time-periodic magnetic flux $a(t)=a_0+a_1(t)$ with the angular frequency ω. Similar to our previous work, where we have considered a static magnetic flux a_0, the electron positions are expressed in terms of collective and relative coordinates. Strong e-e interaction can then be treated in a harmonic approximation for the relative motion. The presently searched solutions of the time-dependent Schrödinger equation for a time-periodic flux are given by the Floquet states. The Floquet states for a spatially constant one-particle potential form a complete set of Floquet-basis states, which is used to study the influence of the one-particle potential on the electronic states. While for a spatially constant one-particle potential the time-averaged observables, such as the electronic energy and the electronic current or angular momentum, depend solely on the time-averaged magnetic flux a_0, a spatially varying one-particle potential leads to pronounced resonances. In the case of moderate electronic relaxation, the stationary properties are determined by the Floquet state with lowest time-averaged energy. For the associated persistent angular momentum we predict jumps with heights proportional to the number of electrons N. We further show that, already by measuring the locations of these jumps in the (a_0,ω) plane, one could determine the number of electrons N as well as the effective e-e interaction.

DOI: 10.1103/PhysRevB.67.165305 PACS number(s): 73.22.Lp, 73.23.Ra, 73.21.−b

I. INTRODUCTION

Mesoscopic rings are the simplest systems revealing electronic quantum coherence in conjunction with the Aharonov-Bohm effect. Their electronic properties have been discussed by many authors. Already two decades ago, Büttiker, Imry, and Landauer[1] have shown that the electronic ground state of a strictly one-dimensional metallic ring enclosing a static magnetic flux carries a flux-dependent persistent current. Being associated with the electronic ground state, this current is expected to survive moderate inelastic backscattering[2–4] as well as elastic backscattering by a spatially varying one-particle potential.[1] These theoretical predictions have been confirmed experimentally by several groups.[5–13] The most recent review of the actual situation is found in Ref. 9. In agreement with the theoretical predictions, the oscillations of the persistent current found for single rings have the period $\Phi_0=h/e$.[6–8] The magnetic response of large ensembles of rings shows oscillations with period $\Phi_0/2$.[5,12,13] The suppression of the Φ_0 periodicity can be attributed to ensemble averaging,[3,4,14] an explanation confirmed by the observed magnetic response of ensembles containing only few rings, where both Φ_0 as well as $\Phi_0/2$ oscillations are found.[10,11]

In spite of the above-described success of the theoretical description of the electronic ground-state properties of mesoscopic rings, some experimental features are not yet well understood. Thus, until now it is not possible to predict the sign of the current at a given flux. Experimentally, the sign of the $\Phi_0/2$ oscillations found for the ensemble-averaged persistent currents corresponds to a diamagnetic behavior for small magnetic fields.[5] Theoretical predictions for a purely one-dimensional ring show that the sign of the current at a given flux depends critically on the spin configuration of the electronic ground state.[15–17] Clearly, when comparing the experiment with these theoretical predictions one has to be aware of the fact that, due to their finite thickness, the rings studied experimentally contain a large number of transport channels and that the experiments are carried out at finite temperatures. Nevertheless, the role of the spin configuration should remain important also in this case.

Another problem concerns the experimentally observed amplitudes of the persistent currents, which have given rise to intense discussion in the literature. The currents in metallic loops are by two to three orders of magnitude too large in comparison with the theoretical predictions based on the one-electron theory.[5,6,10,12] Apparently, the backscattering of electrons by impurities is largely overestimated in these approaches. It is interesting to note that such discrepancies are not found for semiconductor rings.[7,11,13]

Motivated by the failure of the one-electron picture to explain the observed large amplitudes of the persistent currents in metallic loops, several authors have studied the role of e-e interaction. Screening of the Coulomb part of the impurity potentials is important in metal rings and may partly be responsible for the reduced electron backscattering.[18] The particular effects of electronic correlation on the persistent currents have been discussed in Refs. 15–17 and 19–24. A somewhat different explanation of the large amplitudes of the persistent currents has been proposed in Refs. 9, 25, 26, where the dc magnetic response of disordered ring systems is related with the dephasing by internal or external nonthermal equilibrium noise. In this picture, the contributions of excited states become important, i.e., the persistent currents are not a property of the electronic ground state. But e-e interactions remain essential also here, since they determine the coupling of the electronic system to the fluctuating electromagnetic field.[25]

The above-cited theoretical investigations were focused on the magnetic response of ring systems to a *static* external flux. Temporal fluctuations of the electromagnetic field have only been considered to explain the large amplitudes of the persistent currents in mesoscopic metal rings.[9,25,26] In these

studies it was assumed that the amplitudes of the fluctuating electromagnetic fields are small enough to be treated in second order. In the present work we propose a general and systematic approach that allows us to treat the influence of a time-periodic magnetic flux on the electronic states of mesoscopic rings. The influence of time-periodic flux oscillations on systems of strongly interacting electrons is undoubtedly interesting in its own right. In particular, such measurements should give more insight into the particular nature of the electronic correlations. Experimentally, no frequency dependence is observed in the low-frequency range of $10-10^3$ Hz. This is quite expected, since the time variations are very slow in comparison with the relevant dephasing times, so that the electronic system always relaxes into its static ground state (see, e.g., Ref. 5). However, experiments in the interesting high-frequency range should now be feasible. The magnetic response of an ensemble of 10^5 rings etched in a GaAs-AlGaAs heterostructure has recently been measured for an oscillation frequency of 350 MHz.[13] Pieper *et al.*[27] have measured the magnetoconductance of single mesoscopic Ag rings connected to leads, for a time-periodic flux in the frequency range of 250 Hz–1.2 GHz superposed to a static flux. More generally, we expect that the understanding of the behavior of electronic states in a time-periodic flux will also be useful to get a better insight into the effects of nonperiodic fluctuating electromagnetic fields treated in Refs. 9, 25, 26.

Our approach is based on our previous work in Ref. 24, where we have treated the situation of a loop enclosing a static magnetic flux using a continuous real-space representation. Here we will generalize this description by allowing for an additional time-periodic flux. The adequate Hilbert space, the Hamiltonian, and the angular momentum operator for the N-electron system are introduced in Sec. II. The electronic states are described using Floquet's theorem. In Sec. III we derive a solution for the Floquet states. We further introduce the expressions for the time-averaged quantities as for the energy and for the expectation value of the angular momentum, thus completing the description of isolated rings. Under real conditions, coupling with the statistical environment will always lead to electronic relaxation. The relevant time scales and the consequences of relaxation are discussed in Sec. IV. For sufficiently weak interaction with the statistical environment and temperatures $T\to 0$, we find that the stationary situation reached after relaxation is described by the Floquet state with the smallest time-averaged energy. The corresponding time-averaged expectation value of the angular momentum measures the time-averaged ''persistent current.'' In Sec. V we present our numerical results for the time-averaged persistent angular momentum. The resonance features due to the coupling with the time-periodic flux are analyzed. Final conclusions are drawn in Sec. VI.

II. GENERAL THEORETICAL DESCRIPTION

In Ref. 24 we have discussed the situation of N electrons in a circular loop enclosing a static magnetic flux. Presently, we generalize our approach to a time-periodic magnetic flux. We consider N interacting electrons in a circular one-dimensional loop with radius R. A description in polar coordinates is therefore adequate (Fig. 1). Internal and external fields are represented by a time-independent one-particle potential $V(\theta)$ and by a time-periodic tangential vector potential $\vec{A}=A(t)\vec{e}_\theta$ with period P, where the latter corresponds to a time-periodic flux $\Phi(t)$. These potentials satisfy the periodicity conditions

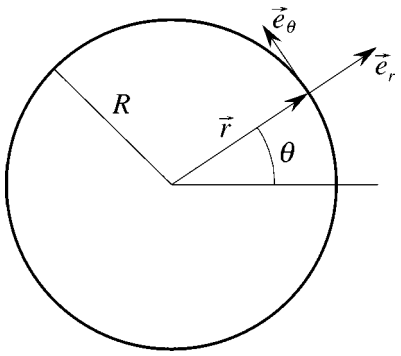

FIG. 1. Geometrical description of the sample system.

$$V(\theta+2\pi)=V(\theta),\quad \Phi(t+P)=\Phi(t)=2\pi RA(t).$$

Expressed in units of the flux quantum $\Phi_0=h/e$, the magnetic flux reads

$$a(t)=\frac{\Phi(t)}{\Phi_0}=a_0+a_1(t),\quad a_0=\frac{1}{P}\int_0^P a(t)dt,$$

where a_0 represents the time-averaged (or static) contribution. We then have

$$\frac{1}{P}\int_0^P a_1(t)\,dt=0.$$

The N-electron wave function at a given time t_s is periodic in the angles θ_n, $n=1,\ldots,N$,

$$\Psi(\ldots,\theta_n+2\pi,\ldots,t_s)=\Psi(\ldots,\theta_n,\ldots,t_s),\qquad n=1,\ldots,N. \tag{1}$$

We assume the spin part of the wave function to be symmetric.[28] The spatial part must then be antisymmetric with respect to the permutation of two electrons,

$$\Psi(\ldots,\theta_k,\ldots,\theta_l,\ldots,t_s)=-\Psi(\ldots,\theta_l,\ldots,\theta_k,\ldots,t_s),\quad k\neq\ell. \tag{2}$$

The system is thus described by the Hilbert space $\mathcal{H}$,

$$\Psi(\vec{\theta},t_s)\in\mathcal{H}=\mathcal{P}(L_2([0,2\pi[^N)),$$

$\mathcal{P}$ being the projector on the subspace of the spatially periodic and antisymmetric functions.

Expressed in the units $\hbar^2/(2mR^2)$ for the energy, $2mR^2/\hbar$ for the time and $\hbar$ for the angular momentum, m being the electron mass, the evolution of the wave function $\Psi\in C^1([0,2\pi[^N\times\mathbb{R},\mathbb{C})$ for a given initial condition is obtained from the Schrödinger equation

$$i\partial_t \Psi = H\Psi \tag{3}$$

with the Hamiltonian

$$H = H_0 + H_{ee} + H_{eV}.$$

The Hamiltonian terms read

$$H_0(t) = \sum_{n=1}^{N} [-i\partial_{\theta_n} - a_0 - a_1(t)]^2,$$

$$H_{ee} = \sum_{1 \le n < n' \le N} \frac{\eta^2}{\left|\sin\frac{\theta_n - \theta_{n'}}{2}\right|},$$

$$H_{eV} = \sum_{\nu > 0} v_\nu \sum_{n=1}^{N} e^{i\nu\theta_n} + \text{c.c.}$$

The angular momentum operator is

$$L(t) = \sum_{n=1}^{N} [-i\partial_{\theta_n} - a_0 - a_1(t)].$$

In this energy scale the *e-e* interaction parameter is $\eta^2 = e^2 mR/(\hbar^2 4\pi\varepsilon_0)$, and the νth Fourier component V_ν of the one-particle potential becomes $v_\nu = 2mR^2 V_\nu/\hbar^2$.

III. THE FLOQUET BASIS

We consider a time-periodic Hamiltonian with period P, $H(t+P) = H(t)$. According to Floquet's theorem, a particular solution of the Schrödinger equation (3) can be written as

$$\Psi(\vec{\theta},t) = e^{-i\varepsilon t}\psi_\varepsilon(\vec{\theta},t), \quad \varepsilon \in \mathbb{R}, \psi_\varepsilon(\vec{\theta},t+P) = \psi_\varepsilon(\vec{\theta},t). \tag{4}$$

The functions ψ_ε are elements of the Hilbert space $\mathcal{H}_P$,

$$\psi_\varepsilon \in \mathcal{H}_P = \mathcal{P}_P(L_2([0,2\pi[^N \times [0,P[)),$$

where $\mathcal{P}_P$ is the projector on the subspace of the spatially periodic, antisymmetric, and time-periodic functions. In the following, they are referred to as Floquet states. The Floquet states $\psi_\varepsilon \in C^1([0,2\pi[^N \times [0,P[, \mathbb{C})$ satisfy the equation

$$\varepsilon\psi_\varepsilon = (H - i\partial_t)\psi_\varepsilon. \tag{5}$$

The period P is related to the angular frequency ω,

$$\omega P = 2\pi.$$

An infinite number of eigenvalues and eigenfunctions of Eq. (5) is associated with the same function $\Psi(\vec{\theta},t)$ in Eq. (4). In fact, if ψ_ε is an eigenfunction in Eq. (5) for the eigenvalue ε, then $\psi_{\varepsilon+\lambda\omega} = e^{i\lambda\omega t}\psi_\varepsilon$, $\lambda \in \mathbb{Z}$, is an eigenfunction for the eigenvalue $\varepsilon + \lambda\omega$. Thus, replacing ε by $\varepsilon + \lambda\omega$ in Eq. (4), one obtains the same function Ψ. Without loss of generality we may then choose the zone

$$\varepsilon \in \left[-\frac{\omega}{2}, \frac{\omega}{2}\right[\tag{6}$$

and define the set of modes

$$M_\varepsilon = \{\varepsilon + \lambda\omega\}_{\lambda \in \mathbb{Z}}. \tag{7}$$

The Floquet parameters ε are often called quasienergies. With the scalar product $\langle \cdot | \cdot \rangle$ in $\mathcal{H}$, one forms the scalar product in $\mathcal{H}_P$

$$\langle f|g\rangle_P = \frac{1}{P}\int_0^P dt \langle f|g\rangle,$$

which is the time-averaged value of $\langle f|g\rangle$. The Floquet states ψ_ε form an orthogonal basis in $\mathcal{H}_P$. A general solution of the Schrödinger equation (3) for a given initial condition can always be expressed as

$$\Psi(\vec{\theta},t) = \sum_j c_j e^{-i\varepsilon_j t}\psi_{\varepsilon_j}(\vec{\theta},t),$$

where the index $j \in \mathbb{Z}$ labels the eigenvalues of Eq. (5) within the zone defined in Eq. (6).

The Hamiltonian depends on the time-periodic magnetic flux $a(t) = a_0 + a_1(t)$. The static flux a_0 may be considered as a parameter. Then, for each a_0 we have a set of eigenvalues $\varepsilon_j = \varepsilon_j(a_0)$, $j \in \mathbb{Z}$. Due to the periodicity of the eigenfunctions ψ_ε in the variables θ_n, $n = 1, \ldots, N$, all spectra are periodic in the static flux a_0 with period 1. Indeed, if the angle-periodic eigenfunction ψ_ε is an eigenfunction of Eq. (5) for the flux a_0, the function $\exp(i\delta\Sigma_{n=1}^N \theta_n)\psi_\varepsilon$ is an angle-periodic eigenfunction for the flux $a_0 + \delta$, provided that δ is an integer. Without any loss of generality one may therefore restrict to the interval $a_0 \in [-\frac{1}{2}, \frac{1}{2}[$. The pairs (a_0, ε_j) denote points in the reduced zone Z_{FB}, the "Floquet-Brillouin" zone,

$$(a_0, \varepsilon_j) \in Z_{\text{FB}} = \left[-\frac{1}{2}, \frac{1}{2}\right[\times \left[-\frac{\omega}{2}, \frac{\omega}{2}\right[\subset \mathbb{R}^2.$$

These points define the Floquet bands $\varepsilon_j(a_0), j \in \mathbb{Z}$. Comparing the solutions $\psi = \psi_\varepsilon$ and $\psi' = \psi_{\varepsilon'}$ to Eq. (5) for different time-periodic fluxes $a(t)$ and $a'(t)$, one obtains the general continuity equation

$$\begin{aligned}(\varepsilon - \varepsilon')\overline{\psi}\psi' - i\partial_t(\overline{\psi}\psi') \\ = -\sum_{n=1}^{N} (-i\partial_{\theta_n} + a - a')[\overline{(-i\partial_{\theta_n} - a)\psi}\psi' \\ + \overline{\psi}(-i\partial_{\theta_n} - a')\psi')].\end{aligned} \tag{8}$$

For fluxes $a(t)$ and $a'(t)$ differing only in the static contribution, $a(t) - a'(t) = a_0 - a_0'$, the integration of Eq. (8) over one period and over the angles leads to

$$(\varepsilon - \varepsilon')\langle\psi|\psi'\rangle_P = -(a_0 - a_0')(\langle L\psi|\psi'\rangle_P + \langle\psi|L'\psi'\rangle_P), \tag{9}$$

where L and L' are the angular momentum operators for $a(t)$ and $a'(t)$, respectively. For identical static fluxes $a_0 = a_0'$, Eq. (9) leads to

$$(\varepsilon - \varepsilon')\langle\psi|\psi'\rangle_P = 0.$$

Floquet states ψ and ψ' for different quasienergies are thus orthogonal.

For two Floquet states ψ and ψ' belonging to the same band ε_j, $\varepsilon=\varepsilon_j(a_0)$ and $\varepsilon'=\varepsilon_j(a_0')$, we obtain after dividing of Eq. (9) by $(a_0-a_0')\langle\psi|\psi'\rangle_P$ and performing the limit $a_0'\to a_0$,

$$\langle L\rangle_{P,j}=-\frac{1}{2}\frac{\partial\varepsilon_j}{\partial a_0}, \tag{10}$$

i.e., the slope of the Floquet band $\varepsilon_j(a_0)$ is given by the time-averaged expectation value of the angular momentum.

The Schrödinger equation for the Floquet states, Eq. (5), may be solved in different ways. A first method consists of the direct calculation using a basis of the Hilbert space $\mathcal{H}_P$. It necessitates the diagonalization of rather large matrices. This approach will, however, be useful in a perturbation scheme. A second method is based on the unitary time-evolution operator $U(t,t_0)$, which relates a system state Ψ at time t to the state at time t_0,

$$\Psi(t)=U(t,t_0)\Psi(t_0),\quad\text{with}\quad i\partial_t U=HU,\ U(t_0,t_0)=\mathbb{I}. \tag{11}$$

A solution of the type defined in Eq. (4) taken over one period P satisfies the eigenvalue equation for the Floquet states

$$U(t_0+P,t_0)\psi(t_0)=e^{-i\varepsilon P}\psi(t_0). \tag{12}$$

The unitarity of the evolution operator implies

$$|e^{-i\varepsilon P}|=1.$$

This shows again that the parameters ε are real and that they are defined up to a multiple of the angular frequency ω. To determine the operator $U(t_0+P,t_0)$, it is convenient to approximate the time-dependent flux by a sequence of steps. We then have

$$a_1(t)=\sum_{m=1}^{M} a_{1,m}C_m(t), \tag{13}$$

with

$$C_m(t)=\begin{cases}1 & \text{if } t_{m-1}\leqslant t<t_m\\ & \qquad m=1,\ldots,M.\\ 0 & \text{otherwise,}\end{cases}$$

The Hamiltonian and the angular momentum are thus time independent in each time interval $[t_{m-1},t_m[$. The lengths $\tau_m=t_m-t_{m-1}$ satisfy the condition $\Sigma_{m=1}^{M}\tau_m=P$. For $t\in[t_{m-1},t_m[$, we have

$$H(t)=H_m=H_{0,m}+H_{ee}+H_{eV},$$

$$H_{0,m}=\sum_{n=1}^{N}(-i\partial_{\theta_n}-a_0-a_{1,m})^2,$$

$$L(t)=L_m=\sum_{n=1}^{N}(-i\partial_{\theta_n}-a_0-a_{1,m}),$$

and the evolution operator becomes

$$U(t,t_{m-1})=e^{-iH_m(t-t_{m-1})},\quad t_{m-1}\leqslant t<t_m.$$

The evolution operator over one period $P=t_M-t_0$ is then given by the time-ordered product

$$U(t_0+P,t_0)=e^{-iH_M\tau_M}\cdots e^{-iH_1\tau_1}. \tag{14}$$

The unitarity of the evolution operator is conserved in this time-step procedure. In comparison with the first method, the size of the matrices that must be diagonalized to solve Eq. (12) is reduced, but the number of diagonalizations increases, since we have to solve the static problem in each interval $[t_{m-1},t_m[$. It is evident, that the time-step procedure yields exact results for any physical continuous time-periodic flux, if the time intervals are chosen sufficiently small.

Using Eqs. (11) and (12) for a stationary solution of type (4), we get the time-averaged quantities for the energy and for the expectation value of the angular momentum,

$$\begin{aligned}\langle H\rangle_P&=\frac{1}{P}\int_0^P dt\langle H(t)\rangle\\ &=\frac{1}{P}\sum_{m=1}^{M}\tau_m\langle\psi_\varepsilon(t_0)|U^\dagger(t_m,t_0)H_mU(t_m,t_0)|\psi_\varepsilon(t_0)\rangle\\ &=\frac{1}{P}\sum_{m=1}^{M}\tau_m\langle\psi_\varepsilon(t_0)|H_m|\psi_\varepsilon(t_0)\rangle,\end{aligned} \tag{15}$$

$$\begin{aligned}\langle L\rangle_P&=\frac{1}{P}\int_0^P dt\langle L(t)\rangle\\ &=\frac{1}{P}\sum_{m=1}^{M}\tau_m\langle\psi_\varepsilon(t_0)|U^\dagger(t_m,t_0)L_mU(t_m,t_0)|\psi_\varepsilon(t_0)\rangle.\end{aligned} \tag{16}$$

IV. ELECTRONIC RELAXATION

Up to now we have considered an isolated electronic loop. Real systems are, however, always embedded in some statistical environment. In the following we assume that the environment is maintained near some equilibrium. The effects due to weak dynamical interaction with the environment may be described by decoherence and energy loss of the electronic system. The relaxation time depends on the coupling of the system to the environment as well as on the dynamical properties of the environment. The typical time scale for the fluctuations of the environment near equilibrium is given by the bath-coherence time τ_{env}. In the limit $\tau_{\text{env}}\to 0$ and for sufficiently weak interaction with the electrons the environment acts as an ideal bath, i.e., memory effects can be neglected. The bath-coherence time τ_{env} has to be distinguished from the coherence time τ_{sys} of the electrons in the system, which depends on the dynamical coupling of the system to the statistical environment. In the hypothetical limit $\tau_{\text{sys}}\to\infty$, the electronic system would be completely decoupled from its environment and evolve coherently.

In the following we assume weak dynamical interaction

between the electronic system and its environment. In this case we have $\tau_{\rm env} \ll \tau_{\rm sys}$. If the environment is held at low temperature, a system described by a time-independent Hamiltonian will relax into its ground state, i.e., its electronic properties are determined by the electronic eigenstate with lowest energy.

Presently we consider time-periodic Hamiltonians with period P. For a weak interaction between the electronic system and its environment, the system will evolve coherently over several periods if

$$\tau_{\rm env} \ll P \ll \tau_{\rm sys}. \tag{17}$$

Under this condition, the system is conveniently described in terms of the Floquet states and the expectation values in the static case have to be replaced by their time-averaged values. For low temperatures, the system will then relax into the ''Floquet ground state,'' the Floquet state with lowest time-averaged energy $\langle H \rangle_P$. The time-averaged physical properties are determined by the properties associated with the Floquet ground state. In the following, we will, in particular, investigate the behavior of the time-averaged expectation value of the angular momentum $\langle L \rangle_P$ associated with this Floquet ground state. It will be denoted as persistent angular momentum $L_{\rm pers}$. In the static case, the persistent angular momentum is of course equivalent to the ''persistent current'' discussed in the literature.[1,2]

For a typical value $\tau_{\rm sys} \approx 10^{-10}$ s, the excitation period has to be much smaller to satisfy condition (17) , i.e., $P \ll 10^{-10}$ s. The angular frequency or the energy of the electromagnetic field should thus satisfy the condition

$$\omega \gg 10^{10}\ {\rm s}^{-1}, \quad E = \hbar\omega \gg 10^{-4} e{\rm V},$$

which corresponds to electromagnetic waves with energy in the far-infrared region.

V. N ELECTRONS IN A TIME-PERIODIC MAGNETIC FIELD

In Ref. 24 we have developed an approach allowing to treat a system of N interacting electrons, which are confined on a one-dimensional loop enclosing a time-independent magnetic field. The electronic positions were expressed in terms of a collective (center-of-mass) coordinate u and relative coordinates $\vec{q}$. We have shown that strong e-e repulsion can be treated within a harmonic approximation allowing to study a large number of electrons. The harmonic approximation of the relative motion becomes exact in the limit of infinite e-e interaction parameter η^2. Even though the accuracy deteriorates for decreasing η^2, the low-energy states, which are physically the most relevant, remain still well described for large but finite η^2.

The approach of Ref. 24 provides a convenient basis to handle the present situation of time-periodic magnetic fields. Adopting the time-step procedure described in Sec. III, we have in fact time-independent Hamiltonians in the intervals $t_{m-1} \leqslant t < t_m$ [Eq. (13)]. For sufficiently small one-particle potentials, it is then convenient to take the eigenstates of the Hamiltonian

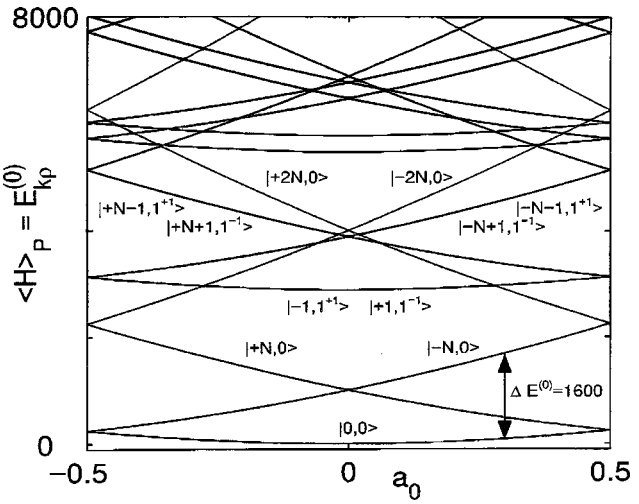

FIG. 2. Energy bands for $N=1001$ interacting electrons in absence of the one-particle potential ($H_{eV}=0$). The e-e interaction parameter is $\eta^2=10^3$. The bands are identified by the eigenstates $|k\varrho\rangle$. The first states of the relative motion are the ground state $\varrho=0$ and the twofold degenerate excitations $\varrho=1^{\pm 1}$ of the first harmonic oscillator with frequency ω_1 (see Ref. 24). Direct dynamical coupling between states k and k' may occur for $k-k'=\nu$ and $v_\nu \neq 0$. The coupling conditions are resumed in Table I.

$$H_{0,m}+H_{ee}=\frac{1}{N}(-i\partial_u - Na_0 - Na_{1,m})^2 + \sum_{j=1}^{N-1}(-\partial_{q_j}^2 + \eta^2\omega_j^2 q_j^2)$$

as a basis (see Ref. 24). Here ω_j denote the frequencies of the harmonic oscillators describing the relative motion of the electrons. The eigenstates of the Hamiltonian may be labeled by $|k\varrho\rangle$, where the indices k and ϱ are associated with the collective and the relative modes, respectively. We have

$$E_{k\varrho}^{(0,m)}|k\varrho\rangle = (H_{0,m}+H_{ee})|k\varrho\rangle,$$

$$E_{k\varrho}^{(0,m)} = \frac{1}{N}(k - Na_0 - Na_{1,m})^2 + \mathcal{E}_\varrho,$$

$$\langle u, \vec{q}|k\varrho\rangle = e^{iku}\varphi_\varrho(\vec{q}).$$

We note that k and ϱ are related due to the symmetry conditions (1) and (2). Since the system is rotationally invariant, the eigenstates $|k\varrho\rangle$ do not depend on the magnetic flux. The corresponding energy bands $E_{k\varrho}^{(0)}(a_0)$ for a static flux $[a_1(t)=0]$ are shown in Fig. 2 for $N=1001$. Considering an additional time-periodic flux $a_1(t)$, we have to look for the time-averaged values given in Eqs. (15) and (16). Up to a constant shift in energy, the time-averaged energy bands remain the same as in the static case. The time-averaged expectation values of the angular momentum are unchanged.

Allowing for a one-particle potential H_{eV}, we express the Hamiltonians $H_m = H_{0,m} + H_{ee} + H_{eV}$ in the basis $\{|k\varrho\rangle\}$. The corresponding matrix elements are

$$\langle k\varrho|H_{0,m}+H_{ee}|k'\varrho'\rangle=\left(\frac{1}{N}(k-Na_0-Na_{1,m})^2+\mathcal{E}_\varrho\right)\delta_{k\varrho}^{k'\varrho'},$$

$$\langle k\varrho|H_{eV}|k'\varrho'\rangle=\sum_{\nu>0}V_{k\varrho}^{k'\varrho'}(\nu),$$

where the matrix elements $V_{k\varrho}^{k'\varrho'}(\nu)$, corresponding to the νth Fourier component of the one-particle potential, have been calculated in Ref. 24. There it was shown that coupling is possible only if

$$|k-k'|=\nu. \tag{18}$$

Note that the matrix elements of H_{eV} are independent of the magnetic flux, so that they can be calculated once for all.

After diagonalization of the Hamiltonians H_m, we can write each factor in Eq. (14) for the time-evolution operator $U(t_0+P,t_0)$ in the common basis $\{|k\varrho\rangle\}$. From Eq. (12) we get the Floquet parameters ε and the corresponding Floquet states $\psi_\varepsilon(t_0)$. The time-averaged energy $\langle H\rangle_P$ and the time-averaged expectation value of the angular momentum $\langle L\rangle_P$ are calculated from Eqs. (15) and (16).

Repeating the procedure for different static contributions a_0, we obtain the Floquet bands $\varepsilon_j(a_0)$ as well as the bands describing the a_0-dependence of $\langle H\rangle_P$, $\langle L\rangle_P$, and of the persistent angular momentum L_{pers}.

Figure 3(a) shows the Floquet bands for $\omega=1600$ and $a_1(t)\equiv 0$. This may be seen as a particular dynamic contribution. To each point (a_0,ε_j) in the Floquet-Brillouin zone Z_{FB} corresponds a time-averaged energy $\langle H\rangle_{P,j}$ [Fig. 3(b)] and a time-averaged expectation value of the angular momentum $\langle L\rangle_{P,j}$ [Fig. 3(c)]. The one-particle potential $v_N=1$ leads to the opening of gaps in the Floquet-band structure, for instance near $a_0=\pm\frac{1}{2}$.

In order to determine the time-averaged persistent angular momentum, we have to identify the Floquet state with the lowest time-averaged energy, the Floquet ground state. The associated Floquet parameters ε are depicted in Fig. 4(a). The corresponding time-averaged persistent angular momenta, calculated from Eq. (16), are shown in Fig. 4(b). In principle, they could also be obtained from the derivatives of the Floquet band [see Eq. (10)]. The time-averaged persistent angular momentum decreases with increasing v_N (see Ref. 24).

In presence of a time-periodic contribution $a_1(t)=a_1\cos(\omega t)$, $a_1\neq 0$, additional gaps due to dynamical coupling appear in the Floquet-band structure at certain static contributions a_0. This is shown in Fig. 5(a). The same dynamical coupling is also at the origin of the rapid changes of the time-averaged energy bands [Fig. 5(b)] and of the time-averaged expectation values of the angular momentum [Fig. 5(c)]. Figure 6(a) shows the Floquet parameters for the Floquet ground states. The associated time-averaged persistent angular momenta given in Fig. 6(b) show well-marked jumps of height N as well as some smaller peaks.

To understand the dynamical effects, it is convenient to choose the eigenstates of the time-periodic operator [see Eq. (5)]

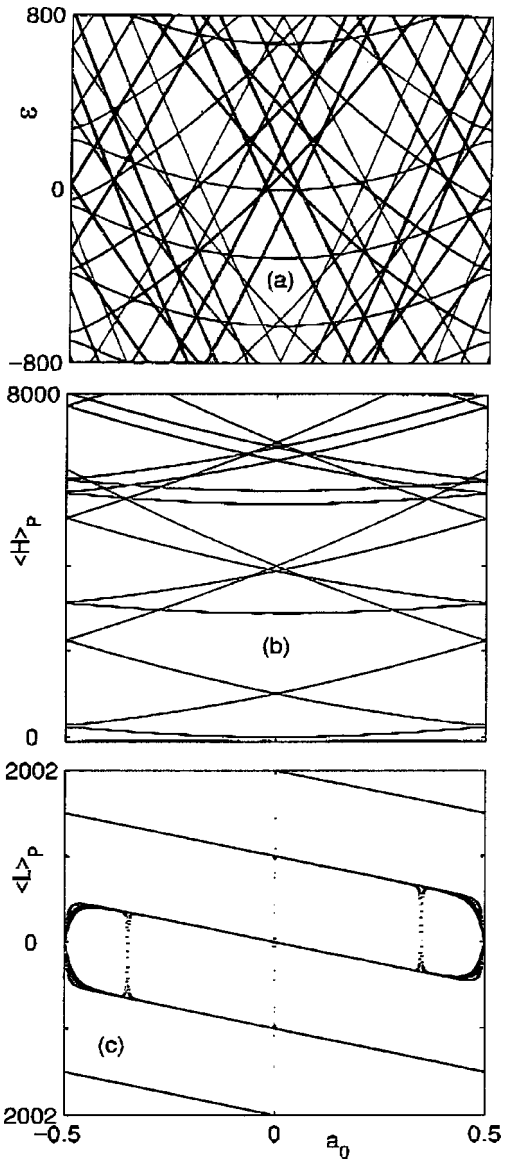

FIG. 3. Dispersion curves for interacting electrons ($N=1001$, $\eta^2=10^3$) in presence of a one-particle potential ($v_N=1$) and a static flux ($\omega=1600$, $a_1=0$): (a) Floquet parameter ε, (b) time-averaged energy $\langle H\rangle_P$, and (c) time-averaged expectation value of the angular momentum $\langle L\rangle_P$. A gap is opened between the first two energy bands $\langle H\rangle_P$.

$$H_0(t)+H_{ee}-i\partial_t=\frac{1}{N}[-i\partial_u-Na_0-Na_1(t)]^2+\sum_{j=1}^{N-1}(-\partial_{q_j}^2+\eta^2\omega_j^2q_j^2)-i\partial_t$$

as an orthonormal basis. The eigenstates may be written as $|k\varrho\lambda\rangle$, where, as previously, the indices k and ϱ label collective and relative modes, respectively, and λ is the Floquet mode index defined in Eq. (7). For the time-periodic contribution $a_1(t)=a_1\cos(\omega t)$, we have the eigenvalues and the corresponding eigenstates

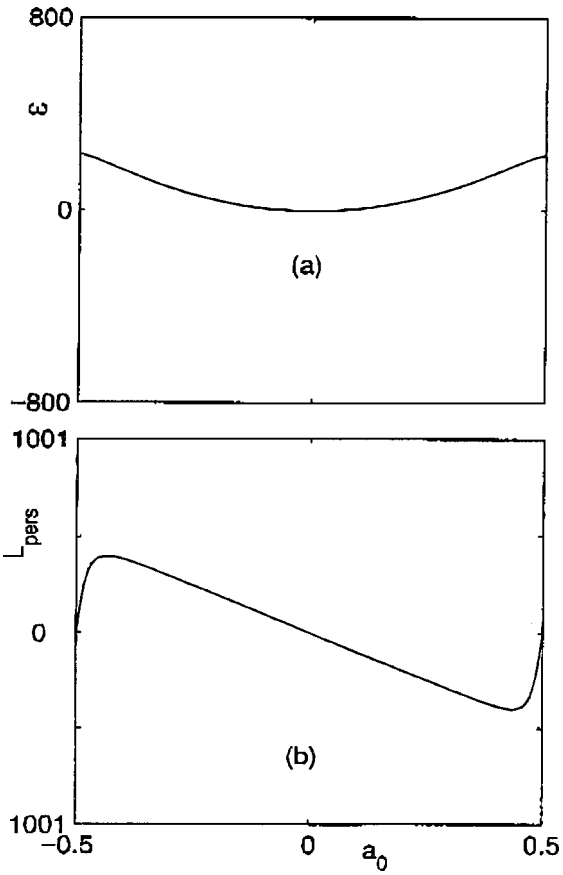

FIG. 4. Dispersion curves for interacting electrons ($N=1001$, $\eta^2=10^3$) in presence of a one-particle potential ($v_N=1$) and a static flux ($\omega=1600$, $a_1=0$) for the Floquet ground state, (a) Floquet parameter ε and (b) persistent angular momentum L_{pers}.

$$E^{(0)}_{k\varrho\lambda}=\frac{1}{N}(k-Na_0)^2+\mathcal{E}_\varrho-\lambda\omega, \tag{19}$$

$$\langle u,\vec{q},t|k\varrho\lambda\rangle=e^{-i\alpha_{k\lambda}(t)}e^{iku}\varphi_\varrho(\vec{q}),$$

$$\alpha_{k\lambda}(t)=\lambda\omega t-\frac{2a_1k}{\omega}\sin(\omega t).$$

From the identity $e^{-iz\sin\phi}=\sum_{s=-\infty}^{\infty}J_s(z)e^{is\phi}$, where $J_s(z)$ are the Bessel functions of the first kind, we get

$$\frac{1}{P}\int_0^P dt e^{i\alpha_{k\lambda}(t)}e^{-i\alpha_{k'\lambda'}(t)}=J_{\lambda-\lambda'}(z_{kk'}),$$

$$z_{kk'}=\frac{2a_1}{\omega}(k-k').$$

The time-averaged energies and the time-averaged expectation values of the angular momentum associated with the basis states $|k\varrho\lambda\rangle$ are

$$\langle H_0(t)+H_{ee}\rangle_P=\langle k\varrho\lambda|H_0(t)+H_{ee}|k\varrho\lambda\rangle$$

$$=\frac{1}{N}(k-Na_0)^2+\mathcal{E}_\varrho,$$

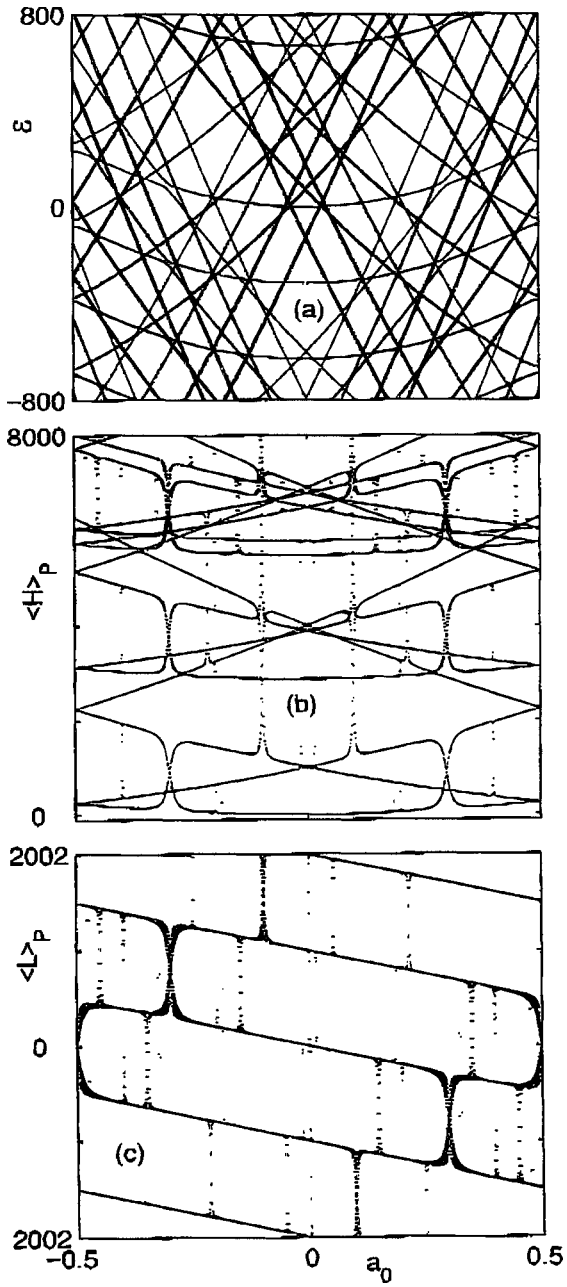

FIG. 5. Dispersion curves for interacting electrons ($N=1001$, $\eta^2=10^3$) in presence of a one-particle potential ($v_N=1$) and a dynamic flux $a_1(t)=a_1\cos(\omega t)$ ($\omega=1600$, $a_1=1$), (a) Floquet parameter ε, (b) time-averaged energy $\langle H\rangle_P$, and (c) time-averaged expectation value of the angular momentum $\langle L\rangle_P$. Due to dynamical coupling between the static bands shown in Fig. 3, additional gaps are opened at Floquet-band crossings leading to the particular behavior of the time-averaged quantities.

$$\langle L\rangle_P=\langle k\varrho\lambda|L|k\varrho\lambda\rangle=k-Na_0.$$

In presence of a one-particle potential H_{eV}, the Floquet states are solutions of

$$\varepsilon|\psi_\varepsilon\rangle=[H_0(t)+H_{ee}-i\partial_t+H_{eV}]|\psi_\varepsilon\rangle.$$

They may be expressed in the above basis as

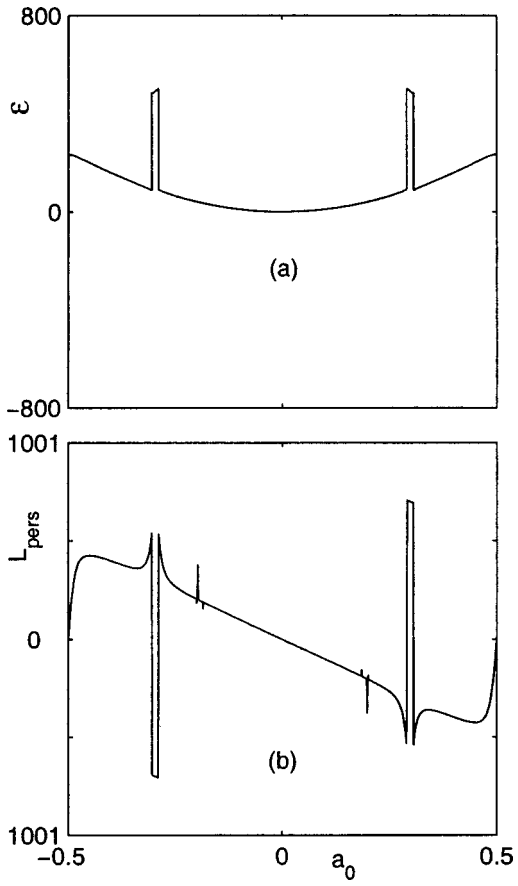

FIG. 6. Dispersion curves for interacting electrons ($N=1001$, $\eta^2=10^3$) in presence of a one-particle potential ($v_N=1$) and a dynamic flux $a_1(t)=a_1\cos(\omega t)$ ($\omega=1600$, $a_1=1$) in the Floquet ground state, (a) Floquet parameter ε and (b) persistent angular momentum L_{pers}. The time-averaged energy bands cross [Fig. 5(b)], leading to jumps of height N of the persistent angular momentum.

$$|\psi_\varepsilon\rangle=\sum_{k'\varrho'\lambda'}|k'\varrho'\lambda'\rangle\Phi_{\varepsilon,k'\varrho'\lambda'}.$$

The coupling of the basis states $|k\varrho\lambda\rangle$ is described by the matrix elements

$$\langle k\varrho\lambda|H_{eV}|k'\varrho'\lambda'\rangle=J_{\lambda-\lambda'}(z_{kk'})\sum_{\nu>0}V_{k\varrho}^{k'\varrho'}(\nu). \quad (20)$$

This shows that dynamical coupling between basis Floquet states with $|k-k'|=\nu$ requires the presence of nonzero Fourier components v_ν.

Taking the limit $a_1/\omega\to 0$, we recover the static situation discussed in Ref. 24. In this case, we have $z_{kk'}\to 0$ and the matrix elements (20) reduce to

$$\langle k\varrho\lambda|H_{eV}|k'\varrho'\lambda'\rangle\to\delta_\lambda^{\lambda'}\sum_{\nu>0}V_{k\varrho}^{k'\varrho'}(\nu).$$

Thus only the Floquet-basis states with $\lambda=\lambda'$ are coupled. For $\omega\to\infty$, the Floquet parameter ε can be identified with the energy, and we may choose $\lambda=0$.

For $a_1/\omega\neq 0$, coupling between Floquet-basis states with different λ becomes possible, as can be seen from Eq. (20). For Floquet states satisfying condition (18), the coupling is largest when the eigenvalues given by Eq. (19) are degenerate. In other words, coupling may occur when the time-averaged energies $\langle H_0+H_{ee}\rangle_P$ of the interacting electrons differ by a multiple of the angular frequency ω. As shown before [see Eq. (6)], we need only to consider the eigenvalues $E_{k\varrho\lambda}^{(0)}$ in the interval $[-\omega/2,\omega/2[$,

$$-\frac{\omega}{2}\leqslant\frac{1}{N}(k-Na_0)^2+\mathcal{E}_\varrho-\lambda\omega\equiv\varepsilon_{k\varrho\lambda}^{(0)}<\frac{\omega}{2}, \quad (21)$$

which determines the integer λ. We thus have to look for crossings in the Floquet-Brillouin zone Z_{FB} (see Figs. 3 and 5). At the Floquet-band crossing we have $\varepsilon^{(0)}(a_0)=\varepsilon'^{(0)}(a_0)$, which implies

$$-\frac{1}{2}\leqslant a_0=\frac{k^2-k'^2+N(\mathcal{E}_\varrho-\mathcal{E}_{\varrho'})-N(\lambda-\lambda')\omega}{2N(k-k')}<\frac{1}{2}. \quad (22)$$

For a given static flux a_0 and in absence of a one-particle potential, a time-periodic flux $a_1(t)=a_1\cos(\omega t)$ does not influence the time-averaged quantities. In Ref. 24 we have shown that for large e-e interaction only Fourier components v_ν with $\nu=\mu N,\mu\in\mathbb{N}$ lead to significant static coupling. The effects of coupling may be amplified in presence of a time-periodic flux $a_1(t)=a_1\cos(\omega t)$ revealing other Fourier components. In the following, we consider the effects of a time-periodic flux for the cases of strong and weak static coupling, which will be represented by Fourier components $v_N\neq 0$ and $v_1\neq 0$, respectively. We further restrict the discussion on the influence of the couplings involving the ground state. Similar arguments hold for any other state.

The Fourier component v_N of the static potential enables dynamical coupling between basis Floquet states with $|k-k'|=N$. Efficient coupling is expected between the ground state $|k\varrho\rangle=|0,0\rangle$ ($\mathcal{E}_\varrho=0$) and the states $|k'\varrho'\rangle=|\pm N,0\rangle$ ($\mathcal{E}_{\varrho'}=0$), when the crossing condition $E_{k'\varrho'}^{(0)}-E_{k\varrho}^{(0)}=\omega$ is satisfied. For $N=1001$, $\eta^2=10^3$, and $\omega=1600$ (see Fig. 2), we find $\lambda=0$ and $\lambda'=1$ from Eq. (21). Equation (22) yields the Floquet-band crossing positions $(a_0,\varepsilon)=(\pm 0.30, 89.61)$ (see Fig. 3). The resulting width of the gap seen in Fig. 5(a) may be estimated for small v_N in a two-band approximation. For $a_1=1$ and $v_N=1$ we obtain

$$\Delta\varepsilon=2\left|J_{-1}\left(\frac{2a_1N}{\omega}\right)v_NNJ_N\right|=26.34,$$

in good agreement with the numerical result. The numerical factor J_N is defined in Ref. 24. The time-averaged energy bands $\langle H\rangle_P(a_0)$ [Fig. 5(b)] associated with the Floquet bands may differ strongly from the energy bands for the static case [Fig. 3(b)]. In particular, the contributions of the Floquet basis states to the Floquet ground state may change strongly with the time dependence $a_1(t)$ of the flux. This is seen in Fig. 6(a). Because of the symmetry of the band structures, we may restrict our discussions to positive fluxes

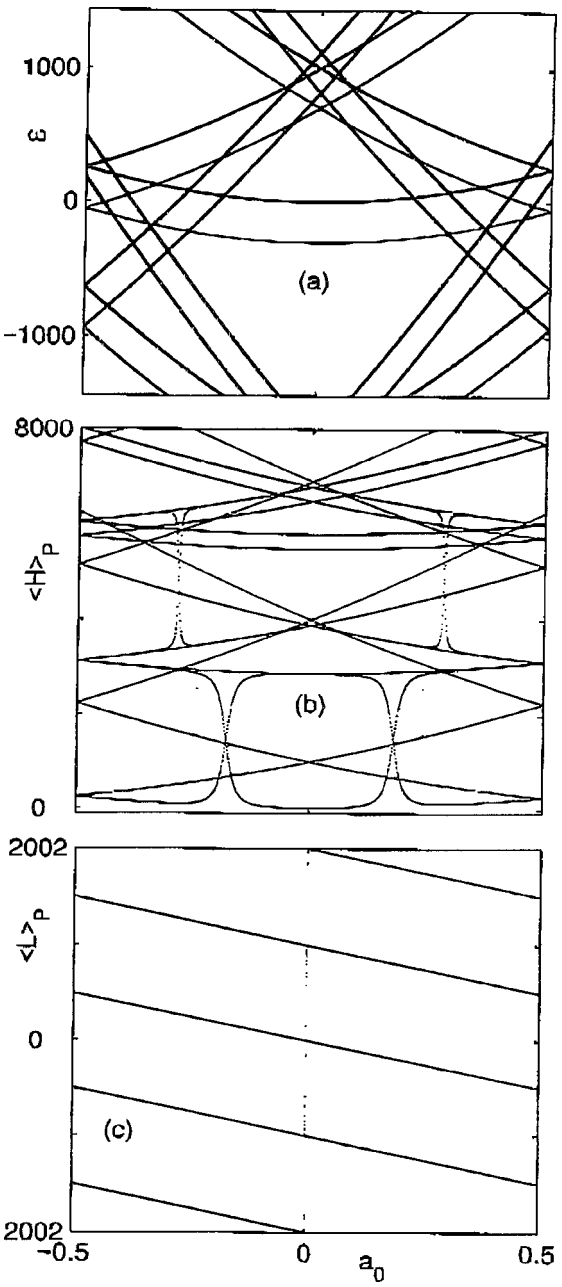

FIG. 7. Dispersion curves for interacting electrons ($N=1001$, $\eta^2=10^3$) in presence of a one-particle potential ($v_1=200$) and a dynamic flux $a_1(t)=a_1\cos(\omega t)$ ($\omega=2885.5<\mathcal{E}_1^{(1)}$, $a_1=1$), (a) Floquet parameter ε, (b) time-averaged energy $\langle H\rangle_P$, and (c) time-averaged expectation value of the angular momentum $\langle L\rangle_P$. The Fourier component v_1 couples between almost identical Floquet bands, leading to the coupling of parallel time-averaged energy bands [Fig. 2(b)].

$a_0\geqslant 0$. Far from the resonance at $a_0=0.30$, the Floquet ground state is essentially described by the Floquet basis state $|0,0,0\rangle$. As in the static case, the associated time-averaged energy is given by $\langle H\rangle_P=Na_0^2$ and the persistent angular momentum is $L_{\text{pers}}=-Na_0$. Near the interval $a_0\in[0.29,\ 0.31]$, coupling with the Floquet basis state $|-N,0,1\rangle$ becomes important, leading to the increase of the absolute value of the persistent angular momentum. In the interval $a_0\in[0.29,\ 0.31]$ the Floquet basis state $|N,0,0\rangle$ gives the main contribution to the Floquet ground state. The time-averaged energy is then given by $\langle H\rangle_P=N(1-a_0)^2$ and the persistent angular momentum is $L_{\text{pers}}=N(1-a_0)$, corresponding to a jump of height N [Fig. 6(b)]. The width of this structure becomes important when the states $k=0$ and $k=\pm N$ are coupled in first order by Fourier components v_N, as is the case in the given situation.

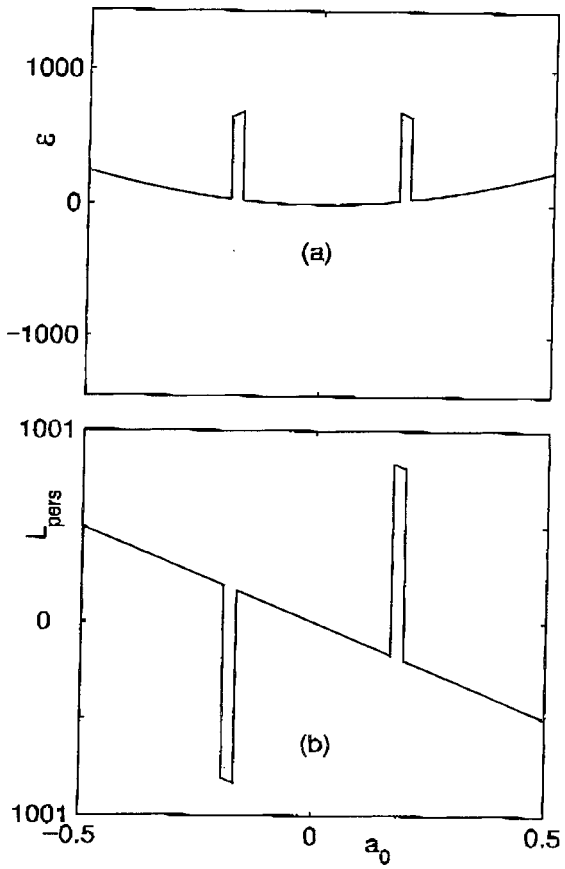

FIG. 8. Dispersion curves for interacting electrons ($N=1001$, $\eta^2=10^3$) in presence of a one-particle potential ($v_1=200$) and a dynamic flux $a_1(t)=a_1\cos(\omega t)$ ($\omega=2885.5$, $a_1=1$) in the Floquet ground state: (a) Floquet parameter ε and (b) persistent angular momentum L_{pers}. The time-averaged energy bands cross [Fig. 7(b)], leading to jumps of height N of the persistent angular momentum.

In principle, the same arguments hold for coupling associated with the Fourier component v_1 of the static potential, which enables dynamical coupling between basis Floquet states with $|k-k'|=1$. Efficient coupling between the ground state $|k\varrho\rangle=|0,0\rangle$ ($\mathcal{E}_\varrho=0$) and the states $|k'\varrho'\rangle=|\pm 1,\ 1^{\mp 1}\rangle$ ($\mathcal{E}_{\varrho'}=\mathcal{E}_1^{(1)}$, see Ref. 24) is expected when the crossing condition $E^{(0)}_{k'\varrho'}-E^{(0)}_{k\varrho}=\omega$ is satisfied. Note that the width of the window for the resonance frequencies

$$-1<\mathcal{E}_1^{(1)}+\frac{1}{N}-\omega<+1$$

is independent of N. For $N=1001$ and $\eta^2=10^3$, we have $\mathcal{E}_1^{(1)}=2885.86$. With the choice of $\omega=2885.5$, we find

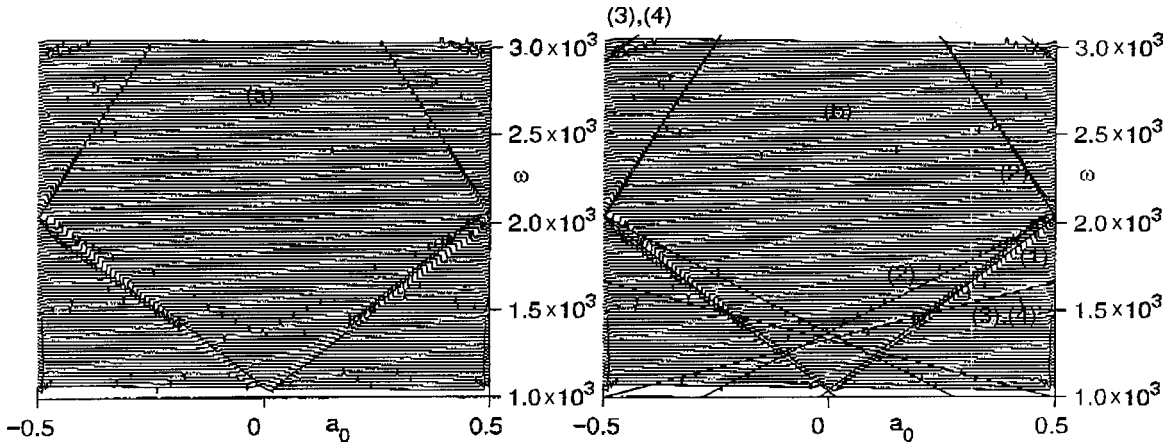

FIG. 9. Persistent angular momentum L_{pers} as a function of the static flux a_0 and the angular frequency ω in presence of a one-particle potential ($v_1=100$, $v_N=1$) and a time-periodic flux ($a_1=1$). The jumps in L_{pers} are located on straight lines in the (a_0,ω) plane, identified in Table I ($\lambda'=1$ and $\lambda'=3$).

$\lambda=0$ and $\lambda'=1$ from Eq. (21). Equation (22) yields the Floquet-band crossing positions $(a_0,\varepsilon)=(\pm 0.18,\ 31.72)$ in agreement with the numerical results shown in Fig. 7. The Fourier component v_1 have to be large to give a sensible effect. Near the interval $a_0\in[0.17,\ 0.19]$, the Floquet basis state $|0,0,0\rangle$ couples with the basis state $|\pm 1,1^{\mp 1},1\rangle$. In contrast to the situation for the v_N coupling discussed above, the time-averaged expectation values of the angular momentum of both states are nearly the same and no additional structures appear in the persistent angular momentum. In the interval $a_0\in[0.17,\ 0.19]$ we obtain again a jump of height N [Fig. 8(b)]. Note that the window for the resonance frequencies is very narrow, and that therefore it will be difficult to observe the jump under realistic experimental conditions.

When both Fourier components v_1 and v_N are present, both the number of electrons N and the first excitation energy $\mathcal{E}_1^{(1)}=2\eta\omega_1$ of the relative motion may be deduced from the positions of the jumps of the persistent angular momentum. Figure 9(a) shows the numerical results for the same set of parameters as before, but the one-particle potential now being described by the two components v_1 and v_N. The resonance structures are seen to follow straight lines, which are identified in Fig. 9(b). The linear dependence can be understood from Table I, where the couplings between the Floquet ground state $|0,0,0\rangle$ and the relevant excited Floquet states $|k'\varrho'\lambda'\rangle$ to first and second order in v_1 and v_N are given. The lines (1) and (2) with slopes $2N$ and $4N$ in Fig. 9(b) correspond to the strongest couplings by v_N for $\lambda'=1$. The lines (2), (3), and (4) with slopes $4N/3$ and $2N/3$ are associated with the weaker coupling for $\lambda'=3$. According to Table I, the position of the quasidegenerate lines (3) and (4) is determined by the first excitation energy $\mathcal{E}_1^{(1)}=2\eta\omega_1$ of the relative motion.

VI. CONCLUSIONS

We have studied the magnetic response of strongly interacting electrons in a one-dimensional loop with respect to a time-periodic magnetic flux. Our approach is based on Ref. 24, where we introduced an explicit basis of N-electron states to describe the situation for strong electron-electron interaction and time-independent potentials. Separating the collective and the relative motion of the N electrons, this basis provides an adequate description of the ground state as well as of the first excitations that can be associated with the excited states of the relative motion.

In the present work, approximating the time dependence of a time-periodic flux by a sequence of piece-wise time-

TABLE I. Floquet states $|k'\varrho'\lambda'\rangle$ coupled with the ground state $|k\varrho\lambda\rangle=|0,0,0\rangle$ to first (v_ν) and second order ($v_\nu v_{\nu'}$), and band-crossing conditions. The energy bands are presented in Fig. 2.

k'	$\mathcal{E}'$	v_ν	a_0	Frequency range
$\pm N$	0	$v_{\mp N}$	$\pm\left(\frac{1}{2}-\frac{\lambda'\omega}{2N}\right)$	$0\leqslant\lambda'\omega\leqslant 2N$
$\pm 2N$	0	$v_{\mp N}v_{\mp N}$	$\pm\left(1-\frac{\lambda'\omega}{4N}\right)$	$2N\leqslant\lambda'\omega\leqslant 6N$
$\pm(1-N)$	$\mathcal{E}_1^{(1)}$	$v_{\mp 1}v_{\pm N}$	$\pm\left(\frac{N-1}{2N}+\frac{\mathcal{E}_1^{(1)}-\lambda'\omega}{2(N-1)}\right)$	$\mathcal{E}_1^{(1)}+\frac{1-N}{N}\leqslant\lambda'\omega\leqslant\mathcal{E}_1^{(1)}+\frac{(1-N)(1-2N)}{N}$
$\pm(1+N)$	$\mathcal{E}_1^{(1)}$	$v_{\mp 1}v_{\mp N}$	$\pm\left(\frac{N+1}{2N}+\frac{\mathcal{E}_1^{(1)}-\lambda'\omega}{2(N+1)}\right)$	$\mathcal{E}_1^{(1)}+\frac{1+N}{N}\leqslant\lambda'\omega\leqslant\mathcal{E}_1^{(1)}+\frac{(1+N)(1+2N)}{N}$

independent fluxes, we have made use of the basis constructed in Ref. 24 for each time interval. We have further assumed the electronic coherence time to be much larger than the period of oscillation. We then have discussed the time-averaged expectation value of the angular momentum, which is equivalent to the time-averaged current. In absence of a one-particle potential H_{eV}, a time-periodic contribution to the magnetic flux has no effect on the time-averaged current and the current equals the free-electron current. As shown in Ref. 24, the *e-e* interaction tends to suppress the backscattering due to the Fourier components v_ν of H_{eV} with noninteger ν/N, while the influence of Fourier components $v_{\mu N}$, $\mu \in \mathbb{N}$, is enhanced. In presence of a one-particle potential H_{eV}, a time-periodic magnetic flux reveals other Fourier components than $v_{\mu N}$ as for example v_1, which would correspond to a static electric field in the plane of the loop. The dynamical coupling leads to additional coupling between Floquet basis states separated in energy by a multiple of the frequency ω. Taken as a function of the time-averaged magnetic flux a_0, the persistent current, which corresponds to the Floquet state with the lowest time-averaged energy, shows jumps of height N. The heights and the positions of the jumps are directly related to the number of electrons and to the first excitation energy of the relative motion, the plasma frequency.

Experimentally, it should, in principle, be feasible to observe the here discussed resonances of the persistent angular momentum by measuring the associated magnetic momentum in presence of time-periodic fields with frequencies in the far infrared. Our results show that such measurements are expected to give useful information about the importance of the *e-e* coupling, the disorder potential, as well as the number of electrons in small ring systems. In order to test our predictions we suggest to look for the appearance of resonances in the (a_0, ω) plane, i.e., to establish the situation of Fig. 9. Since the required Fourier coefficients v_N of the one-particle potential are most probably rather negligible in metals,[24] we expect that semiconductor loops are more interesting for such investigations. The position of the resonances depending critically on the number of electrons N and the loop dimensions, it would also be more indicated to perform such experiments on single rings rather than on ensembles of rings.

ACKNOWLEDGMENT

This work was partly supported by the Swiss National Science Foundation under Grant Nos. 20-52183.97, 20-58972.99, and 20-066681.01.

[1] M. Büttiker, Y. Imry, and R. Landauer, Phys. Lett. **96A**, 365 (1983).
[2] R. Landauer and M. Büttiker, Phys. Rev. Lett. **54**, 2049 (1985).
[3] H.F. Cheung, Y. Gefen, E.K. Riedel, and W.H. Shih, Phys. Rev. B **37**, 6050 (1988).
[4] E.K. Riedel and F. von Oppen, Phys. Rev. B **47**, 15 449 (1993).
[5] L.P. Lévy, G. Dolan, J. Dunsmuir, and H. Bouchiat, Phys. Rev. Lett. **64**, 2074 (1990).
[6] V. Chandrasekhar, R.A. Webb, M.J. Brady, M.B. Ketchen, W.J. Gallagher, and A. Kleinsasser, Phys. Rev. Lett. **67**, 3578 (1991).
[7] D. Mailly, C. Chapelier, and A. Benoit, Phys. Rev. Lett. **70**, 2020 (1993).
[8] R.A. Webb, S. Washburn, C.P. Umbach, and R.B. Laibowitz, Phys. Rev. Lett. **54**, 2696 (1985); V. Chandrasekhar, M.J. Rooks, S. Wind, and D.E. Prober, *ibid.* **55**, 1610 (1985).
[9] P. Mohanty, Ann. Phys. (Berlin) **8**, 549 (1999).
[10] E.M.Q. Jariwala, P. Mohanty, M.B. Ketchen, and R.A. Webb, Phys. Rev. Lett. **86**, 1594 (2001).
[11] W. Rabaud, L. Saminadayar, D. Mailly, K. Hasselbach, A. Benoît, and B. Etienne, Phys. Rev. Lett. **86**, 3124 (2001).
[12] R. Deblock, R. Bel, B. Reulet, H. Bouchiat, and D. Mailly, Phys. Rev. Lett. **89**, 206803 (2002).
[13] R. Deblock, Y. Noat, B. Reulet, H. Bouchiat, and D. Mailly, Phys. Rev. B **65**, 075301 (2002).
[14] B.L. Altshuler, A.G. Aronov, and B.Z. Spivak, Pis'ma Zh. Eksp. Teor. Fiz. **33**, 101 (1981); D.A. Browne, J.P. Carini, and S.R. Nagel, Phys. Rev. Lett. **55**, 136 (1985); A.D. Stone and Y. Imry, *ibid.* **56**, 189 (1986); M. Murat, Y. Gefen, and Y. Imry, Phys. Rev. B **34**, 659 (1986); N. Trivedi and D.A. Browne, *ibid.* **38**, 9581 (1988); G. Montambaux, H. Bouchiat, D. Sigeti, and R. Friesner, *ibid.* **42**, 7647 (1990); B.L. Altshuler, Y. Gefen, and Y. Imry, Phys. Rev. Lett. **66**, 88 (1991).
[15] F.V. Kusmartsev, J. Phys.: Condens. Matter **3**, 3199 (1991); F.V. Kusmartsev, Phys. Lett. A **161**, 433 (1992); **232**, 135 (1997); **251**, 143 (1999).
[16] F.V. Kusmartsev, J.F. Weisz, R. Kishore, and M. Takahashi, Phys. Rev. B **49**, 16 234 (1994).
[17] F.V. Kusmartsev, Phys. Rev. B **52**, 14 445 (1995).
[18] A. Schmid, Phys. Rev. Lett. **66**, 80 (1991).
[19] V. Ambegaokar and U. Eckern, Phys. Rev. Lett. **65**, 381 (1990); V. Ambegaokar and U. Eckern, *ibid.* **67**, 3192 (1991); U. Eckern and A. Schmid, Europhys. Lett. **18**, 457 (1992); G. Vignale, Phys. Rev. B **50**, 7668 (1994); G. Montambaux, J. Phys. I **6**, 1 (1996).
[20] A. Müller-Groeling, H.A. Weidenmüller, and C.H. Lewenkopf, Europhys. Lett. **22**, 193 (1993); A. Müller-Groeling and H.A. Weidenmüller, Phys. Rev. B **49**, 4752 (1994).
[21] P. Schwab, Eur. Phys. J. B **18**, 189 (2000).
[22] K. Niemelä, P. Pietiläinen, P. Hyvönen, and T. Chakraborty, Europhys. Lett. **36**, 533 (1996).
[23] V. Ferrari and G. Chiappe, J. Phys.: Condens. Matter **8**, 8583 (1996).
[24] G. Burmeister and K. Maschke, Phys. Rev. B **65**, 155333 (2002).
[25] V.E. Kravtsov and B.L. Altshuler, Phys. Rev. Lett. **84**, 3394 (2000).
[26] P. Kopietz, A. Völker, Eur. Phys. J. B **3**, 397 (1998).
[27] J.B. Pieper and J.C. Price, Phys. Rev. Lett. **72**, 3586 (1994).
[28] The results presented in this paper remain virtually the same for a different symmetry of the spin function. One then obtains a shift of the dispersion curves with respect to the time-averaged magnetic flux a_0.